Environmental Advances 24 (2026) 100698

Contents lists available at ScienceDirect

Environmental Advances

journal homepage: www.sciencedirect.com/journal/environmental-advances

Combining soil microbial communities and greenhouse gas fluxes along a salinity gradient in temperate Mediterranean coastal wetlands

Emilia Chiapponi, Beatrice Maria Sole Giambastiani *, Nicolas Greggio, Denis Zannoni, Sonia Silvestri, Alessandro Buscaroli, Alessandro Piazza, Federica Costantini

Biological, Geological and Environmental Sciences Department, University of Bologna, Ravenna Campus, Italy

ARTICLE INFO

Keywords:
Temperate coastal wetlands
Microbial communities
Greenhouse gases (GHGs)
Salinity
16SrRNA metabarcoding
Carbon cycle
North adriatic

ABSTRACT

Coastal wetlands play a critical role in carbon sequestration, biogeochemical cycling, and ecosystem stability. These habitats support diverse microbial communities that regulate organic matter decomposition and greenhouse gas fluxes, influencing climate-related feedback mechanisms. However, rising sea levels and saltwater intrusion may disrupt microbial processes, particularly those associated with the sulfur cycle and methane dynamics. Here, we characterize soil physicochemical properties and microbial communities along a salinity gradient in three temperate coastal wetlands to assess the impact of salinity on organic matter decomposition and greenhouse gas emissions. Using full-length Oxford Nanopore MinION 16S rRNA amplicon sequencing, we analyzed microbial communities across freshwater, brackish, and saline wetland soils. Our results indicate that sulfur-reducing bacteria dominate salinized sites, while brackish environments are characterized by obligate anaerobic taxa involved in sulfate reduction, fatty acid degradation, and denitrification. These microbial assemblages contribute to lower CH_4 emissions but increased CO_2 fluxes in the brackish areas, highlighting key microbial-mediated trade-offs in wetland carbon cycling. By integrating microbial diversity, and metabolic functions with soil geochemistry, this site-specific but ecologically meaningful case study improves our understanding of microbe-soil interactions in temperate wetland ecosystems facing increased salinization due to climate change.

1. Introduction

Coastal vegetated wetlands are transitional ecosystems found at the edge of terrestrial and marine habitats. The amount of carbon, also defined as "blue carbon", stored in coastal wetland soils is estimated to equal 25 Pg at the global scale (Duarte et al., 2013) and comes from a constant sink of organic matter associated with slow rates of decomposition. Coastal wetlands are among the most efficient ecosystems in terms of carbon sequestration rate, storing 67–215 Tg C yr^{-1} (Hopkinson et al., 2012), thus playing a crucial role in global biogeochemical cycles (IPCC, 2022). Wetland soils are home to diverse microbial communities that are responsible for driving the processes of organic matter breakdown, nutrient cycling, and greenhouse gas (GHG) emissions (Bridgham et al., 2013). The elements that drive microbial metabolism, such as temperature and precipitation, vegetation, hydrology, soil type, and land use (undisturbed vs. disturbed), influence the rates at which organic carbon mineralizes (Bonetti et al., 2021).

Coastal wetlands are increasingly vulnerable to saltwater intrusion due to sea level rises (White and Kaplan, 2017) and change in freshwater flow and availability (Gillanders and Kingsford, 2002; González-Ortegón et al., 2015). Methanogenic, fermentative, and respiratory pathways are only a few of the many archaeal and bacterial metabolic activities that drive the complex processes of organic matter breakdown in these environments (Liang et al., 2023). Even though recent studies evidenced a salinity-driven shift in microbial community composition favoring sulfate reducers and excluding methanogens (Bartlett et al., 1987; Hartman et al., 2024; Poffenbarger et al., 2011; Weingarten et al., 2023; Zhang et al., 2021; Zhao et al., 2023), many new methanogenic archaea were also identified in coastal sediments and marine ecosystems (Chen et al., 2022; Kumari et al., 2025; Wallenius et al., 2025). The sulfur cycle is one of the most important biogeochemical cycles in coastal wetland environments, as it is closely linked to the production and consumption of CH_4. Sulfate reduction, being energetically favored in comparison to fermentative processes and

* Corresponding author.
E-mail address: beatrice.giambastiani@unibo.it (B.M.S. Giambastiani).

https://doi.org/10.1016/j.envadv.2026.100698
Received 12 November 2025; Received in revised form 12 March 2026; Accepted 12 March 2026
Available online 13 March 2026

methanogenesis, plays an important role in diminishing gross CH_4 production, consequently limiting CH_4 emissions into the environment (Capone and Kiene, 1988). The significance of sulfate reduction within coastal wetland soils is well acknowledged, yet the complexities governing its rates and pathways in these specific environments remain a subject of uncertainty (McCuen et al., 2021). Methanogens are known to be outcompeted by sulfate-reducing bacteria (SRB) for electron donors, which can disrupt microbial activity and lower CH_4 production (An et al., 2023). Seawater contains high concentrations of sulfate, and its intrusion into coastal wetlands increases sulfate availability, thereby promoting the growth and activity of sulfate-reducing bacteria. This enhanced sulfate supply further complicates the biogeochemical processes occurring in wetlands (Jørgensen et al., 2019; Weingarten et al., 2023; Zhang et al., 2021).

The balance between rates of sea level rise, sulfate intrusion, and wetland accretion will have strong impacts on the capacity to store and sequester carbon (Candry et al., 2023; Yousefi Lalimi et al., 2018). By the end of the 21st century, coastal shallow ecosystems in temperate and high latitudes will be at moderate to high risk of submergence and erosion under future emission scenarios (IPCC, 2022; Yang et al., 2023), and consequently risk of increased salinization. The overall response of vegetated coastal ecosystems to rising sea levels depends on the diverse interactions among plant growth, sedimentation processes, and inundation (Marani et al., 2010, 2006; Yang et al., 2023). In this context, biogeochemical studies in wetlands are important for understanding the impact of climate change on the ecosystem services provided by these environments, improving water quality, and mitigating climate change through carbon sequestration (Salimi et al., 2021; Trettin et al., 2019).

In a previous study, Chiapponi et al. (2024) analyzed the environmental variables driving CH_4 and CO_2 emissions from temperate coastal wetlands along the Adriatic coast, showing that salinity and water column height are the major limiting factors of CH_4 emissions and uptake in these environments. Building on the GHG flux measurements reported by Chiapponi et al. (2024), this study uses a multidisciplinary approach combining microbial community structure and soil geochemistry to provide an interpretative framework for observed flux regimes. The main objective is to investigate how microbial communities interact with sulfur availability in hydromorphic soils across three temperate coastal wetlands sites strategically located along a salinity gradient within a limited spatial scale. By characterizing microbial composition and soil geochemical properties, we assess the influence of salinity on methanogenic, fermentative, and respiratory pathways involved in organic matter degradation. These biogeochemical patterns are then discussed with regard to GHG emissions. Rather than focusing on instantaneous correlations, this study links variations in microbial communities and soil geochemistry to site-specific GHG flux patterns, where the microbiome represents a functional snapshot of the soil system and the flux measurements reflect the integrated gas exchange behavior of each wetland.

2. Materials and methods

2.1. Study area

The research was conducted in three sites in the province of Ravenna (Italy) (Fig. 1), along the Adriatic coast. The San Vitale pine forest, along with its internal swamp areas, and the Punte Alberete marsh are located 3-5 km inland of the Northern Adriatic Sea on a palaeodune belt system. The area is characterized by the presence of the Piallassa Baiona, a brackish intertidal lagoon, and the entire study area is part of the Po River Delta Natural Park and SCI (Sites of Community Importance) and SPA (Special Protection Areas) under the European environmental special protection directive (Sites of Community Importance – SCI Punte Alberete SCI/SPA IT4070001 and San Vitale pine forest IT4070003 legislation (Council Directive 92/43/EEC; Directive 2009/147/EC).

The area is characterized by a subcontinental temperate climate with

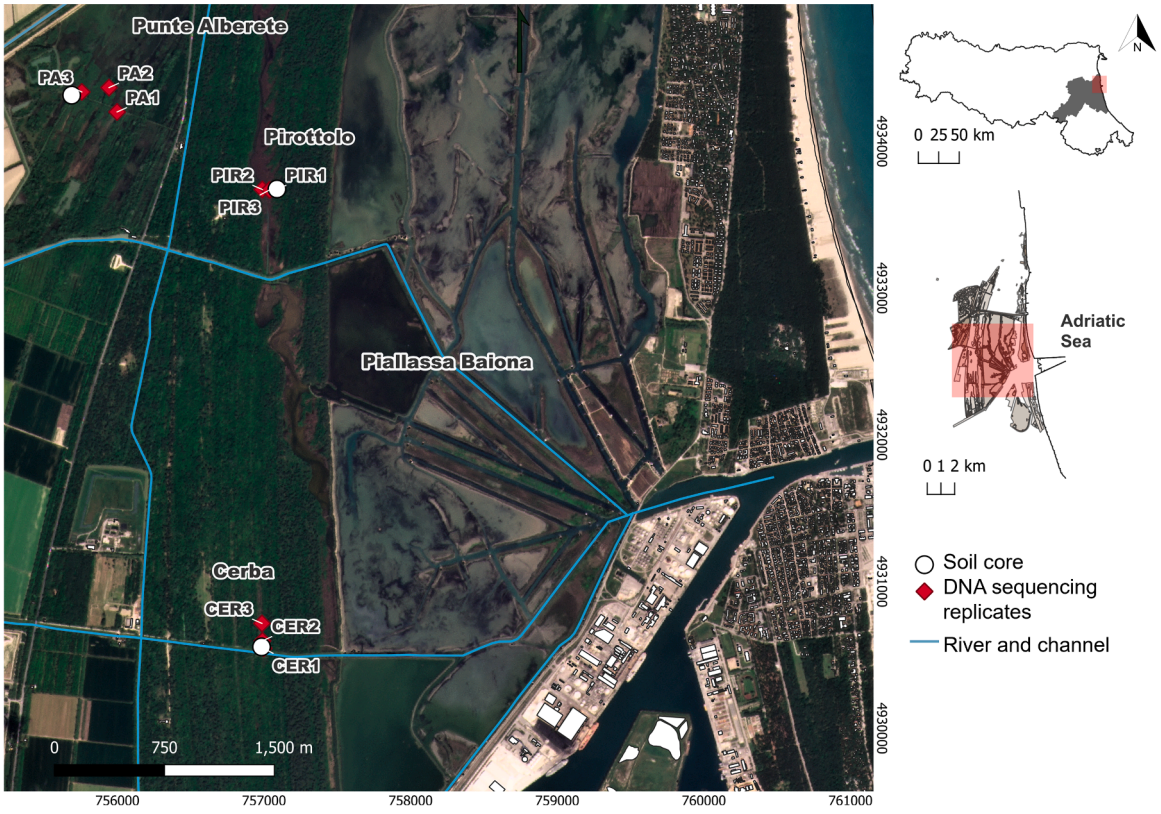

Fig. 1. Study area showing the three temperate coastal wetlands along with the location of sampled cores for molecular and geochemical analysis (coordinate system: EPSG 32632).

about 600 mm of annual rainfall and a monthly mean temperature ranging from 3.6 to 24.3°C in January and July respectively (ARPAE - Regional Agency for Prevention, Environment and Energy of Emilia-Romagna, weather station of Marina di Ravenna https://simc.arpae.it/dext3r/). The coastal area is highly affected by saltwater intrusion due to natural and human-induced factors (Antonellini et al., 2019). The unconfined coastal aquifer consists mainly of sandy deposits, with a finer silt layer at 15-16 m depth (Giambastiani et al., 2007). The only topographical features above sea level are riverbanks, paleo- and coastal dunes, with elevations of 1-3 m a.s.l. The low-lying terrain leads to aquifer salinization, with sporadic freshwater lenses floating on brackish water, and shallow freshwater-saltwater interfaces. During the summer season, high temperatures and low precipitation further reduce aquifer recharge, decreasing the thickness of the freshwater lenses and exacerbating the salinization of both water and soil (Antonellini et al., 2008; Giambastiani et al., 2021).

The entire area is under mechanical drainage that regulates water levels for agriculture, preventing floods but promoting inland saltwater intrusion from the sea and lagoon (Giambastiani et al., 2021). Salinization is particularly severe near Piallassa Baiona lagoon and along canals and rivers connected to the sea (Antonellini et al., 2008). The three selected sites are characterized by a water salinity gradient, ranging from freshwater to slightly brackish to saline waters moving west to east, toward the lagoon. Punte Alberete (PA) is the most freshwater site of the area with a mean annual salinity of 0.7 dS m^{-1} (0.34 ppt); Cerba (CER) is an area characterized by slightly higher salinity, values between 1.4 and 2.2 dS m^{-1} (0.70 – 1.12 ppt); while Pirottolo (PIR) is characterized by brackish EC values of 6-7.1 dS m^{-1} (3.26 – 3.90 ppt) (Chiapponi et al., 2024).

The entire system is human-managed, and the conservation of the wetlands relies on managed water levels, making them more vulnerable to climate change-related threats. The significance of salinity as an ecological process driver in these tidal fresh-/brackish-water wetlands is particularly important given the increase of saltwater intrusion, and its exacerbation in the future scenario due to climate change (Giambastiani et al., 2021, 2020).

Based on regional pedological data from the Emilia-Romagna geoportal (https://geoportale.regione.emilia-romagna.it/catalogo/materiale-cartografico/pubblicazioni/cartografia-e-territorio/pedologia) and previous research in the area (Buscaroli et al., 2009; Buscaroli and Zannoni, 2010; Ferronato et al., 2016), a succession of soils is observed, with topography being the main factor influencing pedogenesis. The alternation of dunes and lowlands determines variations in water table depth with respect to the ground level, strongly conditioning the soil moisture and the salinity degree. Climatic condition, together with the carbonate sandy substrate and spontaneous vegetation land use generate poorly evolved soil profiles with O/A/C horizon sequence, according to the Soil Taxonomy (Soil Survey Staff, 2022). From the dune crests, where the water table is deepest, to the perennially flooded interdune lowlands, the soil morpho-sequence is classified as Psamments, Aquents, and Wassents sub-orders according to the Soil Taxonomy (Soil Survey Staff, 2022). In this area, Aquents and Wassents represent hydromorphic and subaqueous soils respectively in a typical coastal transition system (Ferronato et al., 2016). Seasonal variability also affects the soils of this area: spring and autumn rainfall causes salt leaching from soil horizons, a decrease in the water table depth and its salt content dilution; summer weather conditions cause an increase in water table depth and an increase in soil salinity in surface horizons (Buscaroli and Zannoni, 2017, 2010). Changes in the water table level and the total period of saturation have a significant impact on specific soil-forming processes related to the S cycle, $CaCO_3$ accumulation and depletion, and P and salt concentration (Ferronato et al., 2016).

2.2. GHG emissions measurements

In the same study area, emissions of CH_4 and CO_2 from open standing waters and soils at each site scale were collected once a month from April 2021 to June 2022 using a portable CH_4–CO_2 flux meter equipped with infrared spectrophotometer detectors. Measurements were performed along transects or wetland margins at intervals of approximately 15–20 m. More details about methodology and results are reported in the study of Chiapponi et al. (2024) and for convenience, a summary of the emission rates is provided in Table 1.

During Fall-Winter, CO_2 and CH_4 fluxes varied across sites, with CER showing the highest emissions of both gases (20.34 ± 54.26 g $m^{-2}day^{-1}$ and 61.83 ± 250.44 g $m^{-2}day^{-1}$ of CO_2 and CH_4, respectively), while PA and PIR had lower values. In Spring-Summer, both gases exhibited increased fluxes at all sites, with CER experiencing a substantial rise in CH_4 emissions (mean value of 254.09 ± 549.93 g $m^{-2}day^{-1}$). The coefficient of variation percentage indicates higher variability in CH_4 fluxes across both seasons and all sites. Given this high spatial and temporal variability, GHG flux measurements were integrated over a 14-month monitoring period to obtain site-representative emission patterns, while microbial community and soil geochemical data, collected in a single campaign in June 2022, were interpreted in relation to these flux regimes rather than to instantaneous flux values.

2.3. Core sampling

Cores were collected in June 2022 in four replicates at each sampling site using single-use transparent plexiglass liners (Fig. 2b). Three cores were used for the molecular analysis, while the fourth core was used to perform the geochemical analysis (Fig. 2a). Cores used for microbial characterization were previously disinfected with a solution of 20% NaClO to avoid sample contamination. Each core-liner was inserted in soil ensuring that at least 50 cm of soil was retrieved (Fig. 2b). To avoid oxidation, the headspace was filled with water sampled in the same sampling site and immediately sealed with parafilm and tight stopper. To avoid layer mixing, all the tubes have been ensured in vertical position during transport. In the laboratory, a section of sediment sample was extruded at 0-20 cm for microbial analysis (Fig. 2c) from each core and later preserved at -25°C in sterilized Falcon tubes for DNA extraction. Cores for geochemical analysis were used as a whole and were stored in vertical position at -25°C until performing any pedological analysis.

During core sampling, water temperature (°C), pH, Eh (mV) and EC (dS m^{-1}) were measured at each sampling site using probes logged to an EUTECH datalogger. To assess the influence of salinity on shaping microbial communities, water samples were collected to analyze sulfate (SO_4^{2-}) and sulfide (S^{2-}) concentrations. At each sampling site, a 500 mL water bottle was retrieved without headspace, put in a cooler, and transported to the lab for geochemical analysis, performed on the same day. SO_4^{2-} and S^{2-} concentrations have been measured by using a HACH spectrophotometer (Hach Company, 2019). Moreover, monthly physical-chemical parameters of surface and ground waters were collected for a year at the same sites and published in Chiapponi et al. (2024). These data were also used to support the analysis and discussion.

2.4. Soil characterization

2.4.1. Pedological characterization

Cores were extruded and the soil horizon boundaries were identified and marked. For each horizon, thickness, depth, boundaries, matrix Munsell color (moist), texture, structure, fluidity, coats/film, redoximorphic features, peroxide color change, and presence of organic fragments or roots, were described. After the core extrusion, in water-saturated soil samples, pH, EC, Oxidation-Reduction Potential (ORP), and Acid Volatile Sulfides (AVS) were measured in each horizon. All other analyses were performed on air-dried soil samples. After drying, EC and pH were measured again for all samples in a 1:2.5 (w:v) soil: distilled water suspension. In the latter also soluble nitrates were determined by Ionic Cromatography. For TOC determination, a

Table 1
Summary of CO_2 and CH_4 fluxes measured in the three temperate coastal wetlands by Chiapponi et al. (2024) (Note: n.points = n. point source measured; SD = Standard Deviation; CV(%) = Coefficient of Variation).

Season		Punte Alberete (PA)			Cerba (CER)			Bassa del Pirottolo (PIR)		
		CO_2 (g $m^{-2}day^{-1}$)	CH_4 (g $m^{-2}day^{-1}$)	CH_4/ CO_2 (vol.)	CO_2 (g $m^{-2}day^{-1}$)	CH_4 (g $m^{-2}day^{-1}$)	CH_4/ CO_2 (vol.)	CO_2 (g $m^{-2}day^{-1}$)	CH_4 (g $m^{-2}day^{-1}$)	CH_4/ CO_2 (vol.)
Fall-Winter (Oct-Feb)	**n. points**	80	80		121	121		37	37	
	mean	8.62	7.56	2.41	20.34	61.83	8.34	16.02	1.99	0.34
	SD	13.87	33.67		54.26	250.44		7.83	1.90	
	CV (%)	160.92	445.58		266.77	405.02		48.88	95.70	
Spring-Summer (March-Sept)	**n. points**	122	122		177	177		84	84	
	mean	12.38	6.04	1.34	100.62	254.09	6.93	19.37	15.80	2.24
	SD	17.20	12.65		157.87	549.93		18.11	33.89	
	CV (%)	138.97	209.55		156.90	216.43		93.52	214.52	

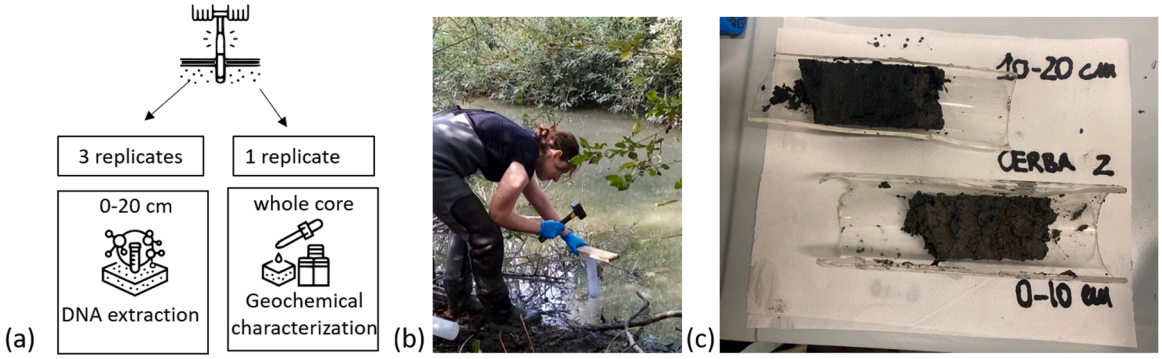

Fig. 2. (a) and (b) Sediment core sampling design at each sampling site using plexiglass tubes (a and b); (c) core sections at different depths extracted in the laboratory for microbial analysis.

carbonates dissolution with 1.5 M HCl was performed before analysis with the elemental analyzer (Thermo Fisher CHNS-O Flash EA 2000) by Dumas flash combustion at 1800°C, while for TN and TH determination this pretreatment was not necessary (ISO, 1995). To determine the presence of sulfidic material, an aliquot of each soil horizon was incubated for 16 weeks after which its pH was measured again according to the Soil Survey Staff (2022) methodology.

2.4.2. *Sulfides from soils*

AVS were determined in sampled cores of soils using a semi-quantitative method proposed by Pellegrini et al. (2018). The blackening of a paper strip, produced by the precipitation of PbS, was compared with a reference table, previously calibrated. The paper sensor method for S^{2-} is very suitable for field screening and has sensitivity levels comparable to laboratory methods. The reference chart was prepared by adding standard S^{2-} solutions ranging from 0.1 to 10 mmol/L following the method suggested by Pellegrini et al. (2018). Paper strips (3 × 6 cm) were cut from Whatman ® N.1 filter paper and impregnated with 6 drops (approximately 0.3 mL) with 1.5 M $Pb(NO_3)_2$ shortly before use. The impregnated area was 3 × 4 cm, with the remaining 3 cm dry for pinching the paper strip to a 250 mL polyethylene jar. An aliquot of 10 mL standard solution on fresh soil was placed in the disruptor tube, provided by the extraction kit. The cap was closed after 50 mL of 6M HCl was added. The jar was then swirled for 15 seconds to ensure thorough contact between the soil and the acid and to speed up H_2S volatilization. The volatilized H_2S combined with the Pb^{2+} on the paper strips to generate PbS, which darkened the paper in proportion to the amount of H_2S developed. The jar was opened after 5 minutes, and the paper strip was removed and immediately compared to the reference colorimetric chart and scanned.

2.4.3. *Sulfur characterization*

Total sulfur and elemental composition were measured from each soil horizon with X-ray fluorescence (XRF). Each aliquot of dried and milled material was pressed in a thin pallet in a boric acid binder and used to analyze the elemental chemistry with an Axios-Panalytical sequential wavelength dispersive XRF spectrometer with a 4 kW Rh tube and SuperQ 3.0 software. Thermogravimetric analysis was carried out using an Eltra Thermostep thermogravimetric analyzer (Eltra GmbH, Haan, Germany) in an oxidant atmosphere (air, 90 mL min^{-1}) at 10°C min^{-1} to 600°C for organic matter determination and then at 25°C min^{-1} to 950°C for carbonate determination (Kasozi et al., 2009).

2.5. *DNA extraction, 16S rRNA gene amplification and sequencing*

From each sampling site and replicate (3 sites, 3 replicates per site), a representative sample of the 0-20 cm core was collected and used for DNA extraction. Total DNA was extracted using the E.Z.N.A.® SOIL DNA KiT (Omega Bio-Tek) inserting 250 mg of the homogenized sample inside the Distruptor Tube provided by the manufacturer. DNA extraction for each sample was performed on the same day together with two negative controls: a tube with only nucleotide-free water and a tube with laboratory aerosol. The latter was prepared by leaving a 2 mL Eppendorf vial open on the laboratory workbench for several hours and later proceeding with the extraction procedure as the biological sample. DNA concentrations were quantified by using the Qubit dsDNA HS As say Kit with a Qubit 2.0 fluorometer (Invitrogen).

The portable DNA sequencer (MinION) from Oxford Nanopore Technologies (ONT) was utilized to characterize the microbial communities (Kerkhof et al., 2017). Following the manufacturer's instructions, sequencing libraries were prepared using the 16S Barcoding Kit (SQK-16S024) from Oxford Nanopore Technologies (ONT), Oxford, UK amplifying ~1500 bp of the 16S V1V9 with the primers: 27F:

5'-TTTCTGTTGGTGCTGATATTGC AGRGTTYGATYMTGGCTCAG-3′ and 1492R: 5'-ACTTGCCTGTCGCTCTATCTTC CGGYTACCTTGTTACGACTT-3' For each sample, 10 ng of DNA was used for PCR amplification. The PCR procedure consisted of 30 cycles of initial denaturation at 95°C for 1 minute, denaturation at 95°C, annealing at 55°C, and extension at 65°C, followed by a final extension at 65°C for 1 minute. Negative PCR controls (PCR reagents without DNA) were amplified at the same time.

Barcoded samples were pooled in equimolar proportions, and about 82 fmol of the pooled sample was loaded into a MinION flow cell (R10.3, FLOMIN111). The flow cell was inserted in the MinION for sequencing and the run, operated by ONT's MinKNOW 4.3.12 software (Oxford Nanopore Technologies, Oxford, UK) lasted for 20 hours and the raw fast5 reads were basecalled and demultiplexed using Guppy v2.3.

Passed reads were analysed using the EPI2ME pipeline (V5.0.2) using the workflow wf_metagenomics (v2.4.1) fully available from EPI2ME repository (https://github.com/epi2me-labs/wf-metagenomics). Taxonomic classification was performed with the integrated Kraken2 classifier (v2.1.3) (Wood et al., 2019) against the ncbi_16s_18s database that contains 16S ribosomal RNA sequences, corresponding to bacteria and archaea type materials. The parameter settings of the workflow were: minimum length filter 1350, maximum length filter 1650, mean quality score ≥ 7, batch size 32000, bracken length 10000, and default values in the remaining parameters. The pipeline of this workflow does not process by default reads in the unclassified directory. Only taxa with more than 9 total reads were included in the phylum- and genus-level abundance data.

To detect metabolic or ecologically relevant functions (i.e., nitrogen fixation, sulfate respiration or hydrocarbon degradation) of the genera retrieved, the database FAPROTAX (Louca et al., 2016) was used. FAPROTAX can be used for a fast-functional screening or grouping of 16S derived bacterial and archaeal data from terrestrial ecosystems (Sansupa et al., 2021). Nevertheless, to increase the information about the ecological function of different genera, literature references and SILVA (Pruesse et al., 2012) and NCBI (Sayers et al., 2022) databases have been used.

2.6. Statistical analysis

To assess whether sequencing depth limited the representation of taxonomic diversity, the DNA sequencing effort was calculated through species accumulation curves on genus-level abundance data with more than 9 total reads using rarecurve() function. For all the samples, stacked histograms representing microbial taxa at phylum and genus levels including their relative abundance were drawn. Prior to the analysis, data were rarefied to the minimum number of reads of any sample using rrarefy() function.

Alpha diversity was calculated for each sampling site (PA, CER, and PIR) on rarefied abundance data at genus level as (1) total taxa richness (S), and (2) Pielou's Evenness index (J) (Pielou, 1966). Pielou's Evenness index estimates the degree of uniformity in the distribution of individuals among different genera. Spatial differences in diversity indices among sites were tested using the aov() function.

Beta diversity analyses were performed on Bray–Curtis dissimilarity matrices obtained with vegdist() after Hellinger-transformed data, without rarefaction. The spatial differences on microbial community structure and functional structure among sites were tested by multivariate permutational analysis of variance (PERMANOVA) using adonis2() function with 9999 permutations. The assumption of homogeneous multivariate dispersion was evaluated using PERMDISP (betadisper(), type = "centroids"), with significance assessed by permutation tests (permutest(), 9999 permutations).

The pattern in the distribution of samples was displayed using the distance-based Redundancy Analysis (dbRDA). Selected environmental variables and CO_2 and CH_4 fluxes were prior standardize using decostand() function, then dbrda() was calculated. Significance of the model, axis, and the environmental variable were also assessed with anova.cca (). Before testing dbRDA model, correlations between environmental variables and fluxes were performed using cor() function with "spearman" method. Variables that correlated have been not used in the dbRDA model.

Similarity percentage (SIMPER) routines (70% cut off; Clarke, 1993), were performed to detect taxa and their metabolic functions that contributed most to similarity within sites and dissimilarity between sites.

All the analyses were performed using R software (version 4.2.2) (Oksanen et al., 2022) with the "vegan" package (version 14 2.6-4), while SIMPER analyses were performed using Primer 7 (Clarke and Gorley, 2015).

3. Results

3.1. Geochemical characterization

The key geochemical parameters of soil horizons are identified in each core (Table 2). The PA soil profile consists of four horizons (Ase, Ag, Cg1, and Cg2) with a transition from silty loam in the upper horizons to silty clay loam in the deeper ones. The total lime content increases with depth and it is the largest at 17-32+ cm with 307 gkg^{-1}. The shallow layer shows the highest pH, EC, TOC, and TN values, as well as S and AVS concentrations and they decline with depth. Overall, PA has the highest ORP values and the lowest AVS values compared to the other sites, suggesting a less reduced environment with lower sulfide content. Based on collected information, this soil profile can be classified as Fluic Frasiwassent, fine-loamy, mixed, calcareous, and mesic (Soil Survey Staff, 2022).

The CER soil profile consists of four horizons (Ase, Ag, Cse, and 2Cse) with a texture ranging from silty loam in the upper layers to sandy loam in the deepest horizon. The total lime content is 283 gkg^{-1} in the superficial horizon and decreases with depth to 118 gkg^{-1}. This profile is characterized by a decrease in ORP with depth, indicating more reduced conditions. The highest AVS and sulfur concentrations are found in the surface and deepest horizons, while Fe follows the opposite trend, with higher concentrations in the middle layers. pH increases with depth, while TOC and TN decrease. Soluble nitrates peak in the intermediate horizons and are nearly absent at the top and bottom. Overall, the CER profile exhibits strong reducing conditions with significant sulfide accumulation at depth. It is classified as Haplic Sulfiwassent, coarse-loamy, mixed, calcareous, and mesic (Soil Survey Staff, 2022).

The PIR soil profile consists of five horizons (Oi/Ase, Ase, A/Cse, Cse, and Cg) with a sandy loam texture at the surface that becomes sandy with depth. The lime content is null at the top horizons and increases to 62 gkg^{-1} in the 31-50+ cm horizon. This profile is characterized by increasing pH, EC, and ORP with depth. TOC and TN are highest in the organic-rich surface layer and decline with depth. AVS concentrations follow a similar trend, being highest at the surface and decreasing in the bottom horizons. Sulfur remains relatively stable except for a decrease in the middle horizon, while iron gradually declines with depth. Overall, the PIR profile shows strong organic matter influence at the surface, and it is classified as Sulfic Psammowassent, mixed, mesic (Soil Survey Staff, 2022).

More details on morphological features of soil profiles are listed in Tab. S1 in the Suppl. Mat.

3.2. Characterization of microbial communities

MinION sequencing of the 8 core sediment samples yields, after read length and quality filters, 2534917 high-quality reads with 0.02% of unclassified reads (replicate PA3 are excluded from the analysis due to its low number of reads, less than 1000). On average, 310254 ± 119265 reads are obtained for PA, 365632 ± 73054 for CER samples, and 257901 ± 123832 reads for PIR. No positive amplification of the PCR-

Table 2
Properties of water-saturated and air-dried soils for different horizons. Each row in the table corresponds to a specific horizon within a soil profile (codes according to Soil Survey Staff, 2022), and the columns present parameters retrieved for both water-saturated and air-dried samples.

			Water-saturated soil analysis				Air dry soil analysis						
Profile	Horizon	Depth	H_2O reaction	EC sp 25°C	Mean ORP	S - AVS	H_2O reaction		EC 1:2.5 25°C	Total lime	TOC	TN	TOC/TN
		cm	**pH**	**dS m^{-1}**	**mV**	**mg kg^{-1}**	**In pH**	**Fin pH**	**dS m^{-1}**	**g kg^{-1}**	**g kg^{-1}**	**g kg^{-1}**	
PA	Ase	0 - 4	7.16	0.85	-86	412	7.30	7.75	1.77	191	100.5	6.30	16.0
	Ag	4 - 10	7.00	0.97	-95	10	7.51	7.71	0.74	144	101.2	5.16	19.6
	Cg1	10 - 17	6.78	1.18	-47	8	7.88	8.01	0.68	231	26.6	2.40	11.1
	Cg2	17 - 32+	7.02	0.96	-68	53	8.11	8.26	0.88	307	13.8	1.46	9.4
CER	Ase	0 - 5	7.37	1.14	-159	1562	7.58	7.74	2.39	283	36.7	3.67	10.0
	Ag	5 - 10	7.27	1.91	-130	174	7.81	7.82	1.52	260	23.5	2.38	9.9
	Cse	10 - 23	7.31	1.44	-223	673	7.96	7.85	1.31	205	11.0	1.21	9.1
	2Cse	23 -35	8.25	1.29	-224	1854	8.56	7.94	0.74	118	2.4	0.24	10.0
PIR	Oi/Ase	0 - 6/7	7.04	5.01	-233	4568	7.26	7.66	7.46	0	119.6	7.14	16.7
	Ase	6/7 - 15	7.43	11.60	-113	1508	7.52	6.96	7.80	0	69.8	4.57	15.3
	A/Cse	15 - 20	7.51	13.80	-77	2461	7.60	7.07	6.03	17	19.5	1.23	15.9
	Cse	20 - 31	7.33	11.80	-198	2168	7.96	6.99	4.27	19	6.5	0.55	11.8
	Cg	31 - 50+	7.34	12.90	-80	658	7.88	7.56	4.79	62	3.4	0.29	11.8

Parameters: AVS = Acid Volatile Sulfides; TOC = Total Organic Carbon; TN = Total Nitrogen; PIR = Pirottolo site; CER = Cerba site; PA = Punte Alberete site. Water reaction on air dried soil is reported before and after the 16 weeks of incubation ('In pH' and 'Fin pH', respectively); **Horizon master:** O = organic horizon; A = surface mineral horizon; C = parent material; I = slightly decomposed material; se = presence of sulfides; g = strong gleying.

negative controls or extraction-negative controls are observed; therefore, they are not sequenced.

Species accumulation curves on genus-level abundance data indicate that the samples reach a plateau, highlighting that sequencing depth is appropriate in all the sample replicates (Fig. S1 in Suppl. Mat.).

3.2.1. Taxonomic composition

The 16S metabarcoding analysis identifies 42 phyla, 648 families and 2354 genera. The most abundant phyla are Pseudomonodata and Thermodesulfobacteriota (Fig. 3a). The most abundant genera are *Thiobacillus, Desulfatiglans*, and *Syntrophus* (Fig. 3b). Sample PA is dominated by genera *Syntrophus* (5.04±1.8%) and *Thiobacillus* (3.8±2.01%). In the CER site, on the contrary, we observe a prevalence of *Thiobacillus* (4.4±1.48%) and *Sulfuricurvum* (2.97±0.89%). In the PIR brackish-water site we observe a different prevalence of taxa compared to the other sampling sites. The most abundant taxa are *Desulfatiglans* (3.55 ±0.71%), and *Desulfosarcina* (1.94±0.56%).

Taxa Richness (Genus level) (S) is not statistically significant different among sites with PA showing an average of 1493±211, CER with 1680±30 taxa, and PIR with 1480±163 taxa (F value=0.701, p>0.05, Tab. S2 in Suppl. Mat., Fig. S2 in Suppl. Mat.). Also mean Pielou's evenness (J) is not statistically significant different among sites (F value=0.819, p>0.05, Tab. S3 in Suppl. Mat., Fig. S3 in Suppl. Mat.).

3.2.2. Community structure and function

The microbial community structures are statistically significantly different among sampling sites (R^2=0.5448, F=2.9916, p<0.05, Fig. 4, Tab. S4 in Suppl. Mat.), while dispersion was not significantly different among the groups (PERMDISP, F=1.3307, p>0.05, Tab. S5 in Suppl. Mat.). Based on the spearman correlation matrix and ecological meaning of the measured environmental variables and CO_2 and CH_4 fluxes, the selected variables for the dbRDA model are EC sp 25°C and ORP (Figs.4 and S4 in Suppl. Mat.).

The clustering of the sample within sites is also evidenced by the dbRDA (Fig. 4). The plot highlights clear clustering patterns, with PA replicate samples positioned closely in the top-left quadrant, CER replicate samples in the bottom-left and PIR replicate samples in the top-right quadrant, showing clear distinct community structures between the three sites. The points distribution on the dbRDA plot are displayed along a salinity range, with freshwater sites on the left quadrant, and brackish sites on the right.

Overall, the dbRDA reveals that EC sp 25°C and ORP together explain 54.5% of the variation in microbial community structure. The overall model is statistically significant (F=2.9916; p <0.05; Tab. S6 in Suppl. Mat.), and both constrained axes are individually significant (dbRDA1: F=3.5748, p < 0.05; dbRDA2: F=2.8901, p < 0.05; Tab. S7 in Suppl. Mat.). The first axis (dbRDA1) explains 32.5% of the total variance, while the second axis dbRDA2) explains 21.9%. Marginal effects tests show that EC sp 25°C independently explains a significant portion in community variation (F=3.4682; p < 0.05; Tab. S8 in Suppl. Mat.), and that ORP also makes a significant contribution (F=2.5091; p < 0.05; Tab. S8 in Suppl. Mat.).

SIMPER analysis reveals that the average similarities of microbial communities among replicates within sampling sites is relatively high: PA 82.87%, CER 83.18%, and PIR 77.03%. Moreover, the dissimilarity between sites is low mainly due to the high number of genera with low abundance and it is 23.61% between CER and PA, 24.98% between CER and PIR, and 27.87% between PIR and PA (data not shown).

FAPROTAX analysis is utilized to evaluate the difference in functional microbial groups within the three sampling sites. Since FAPROTAX is non-exhaustive and many organisms known to perform certain functions may be missing or may only be partially included in the database, we also performed bibliographic research for the most abundant genera (Tab. S9 in Suppl. Mat.). 56 out of 2354 genera (2.38 %) are assigned to at least one functional group. 12 functional groups are represented (i.e., associated with at least one record) (Tab. S10 in Suppl. Mat.), while 6 were excluded from the analysis because they were not related to microbes associated with soils (invertebrate_parasites, human_pathogens_all, human_gut, human_associated, mammal_gut, animal_parasites_or_symbionts). Chemoheterotrophy is the group with the highest number of genera (51), followed by methylotrophy (18), aerobic chemoheterotrophy (17), and metanotrophy, fermentation, and hydrocarbon_degradation, all with 16 genera represented (data not shown).

In terms of relative abundance, the most abundant functional group are Sulfur Oxidation (*Thiobacillus, Sulfovorum, Sulfuricurvum*), Sulfate Reduction bacteria (*Desulfatiglans* and *Desulfosarcina)* and Chemoheterotrophy (Fig. 5). Nevertheless, statistically significant differences are observed in the functional structure among sampling sites (R^2=0.64283, F=4.4995; p < 0.05; Tab. S11 in Suppl. Mat.).

SIMPER analysis indicates high average similarities within sampling site (90.18% in PA, 90.76% in CER and 87.98% in PIR) (Tab. S12 in Suppl. Mat.). Between sampling sites, the average dissimilarity is 15.08% between CER and PIR, 15.68% between PA and PIR, and 17.49% between PA and CER. In PA we observe higher abundance of syntrophic and methanol oxidation bacteria compared to CER and PIR. (Tab. S12 in Suppl. Mat.).

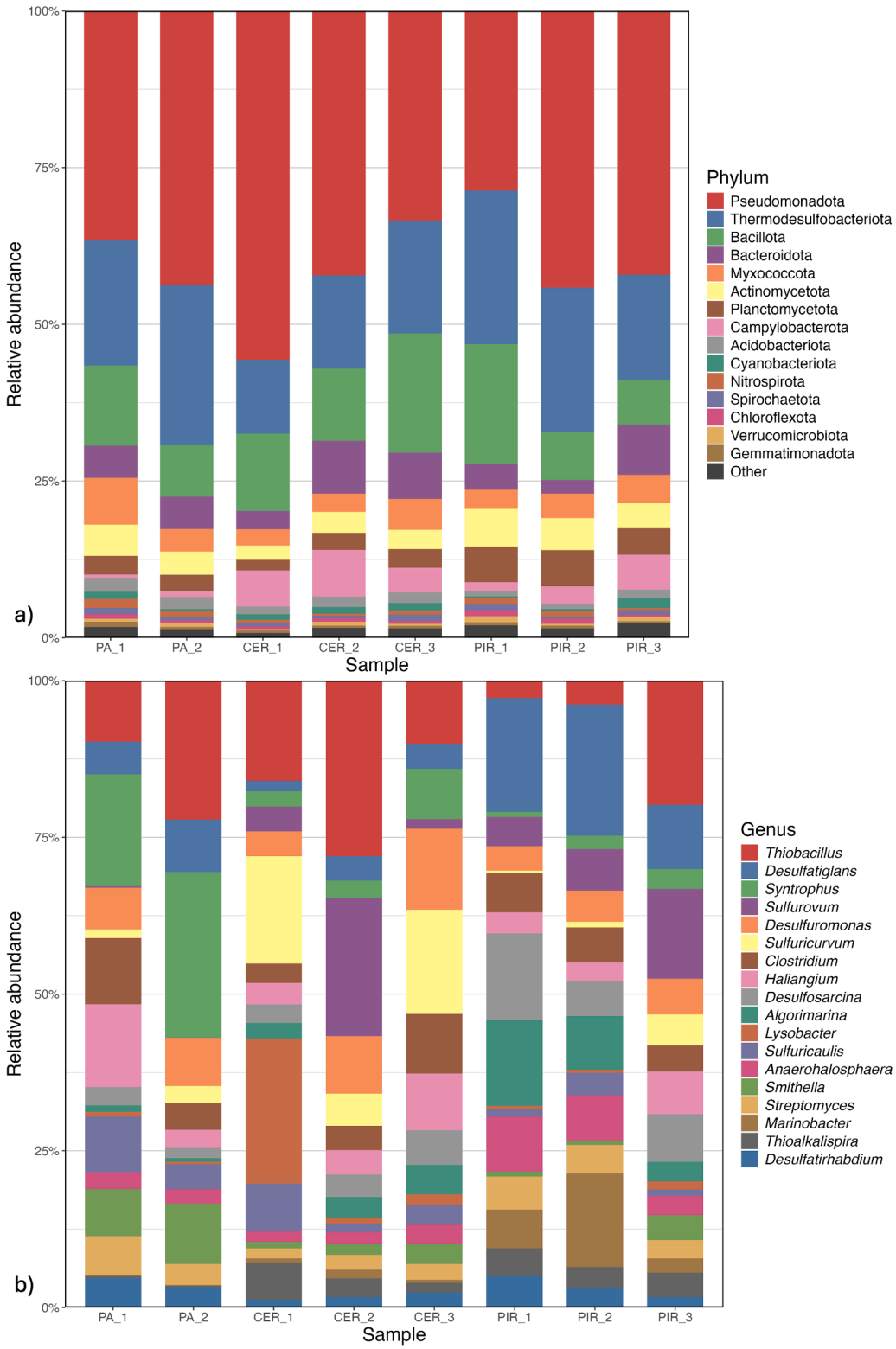

Fig. 3. (a) Relative abundance at phylum rank found in each replicate sample. The term "Other" includes those phyla with total relative abundance < 2%. (b) Relative abundance at genus rank found in each replicate sample. Genera with total relative abundance < 5% were not shown. PA is for Punte Alberete site; CER is for Cerba site; and PIR is for Pirottolo site; replicate PA3 was excluded from the analysis due to its low number of reads.

4. Discussion

The previous work by Chiapponi et al. (2024), performed in the same study sites, found that salinity and water column height play a major role in limiting CH_4 and CO_2 emissions in these coastal wetlands. That study proposed that differences in water column height may modulate CH_4 oxidation, with shallow waters favoring CH_4 diffusion and limiting oxidation, and deeper waters supporting higher oxidation and associated CO_2 production. In the present study, this interpretation is indirectly supported by functional inferences based on FAPROTAX.

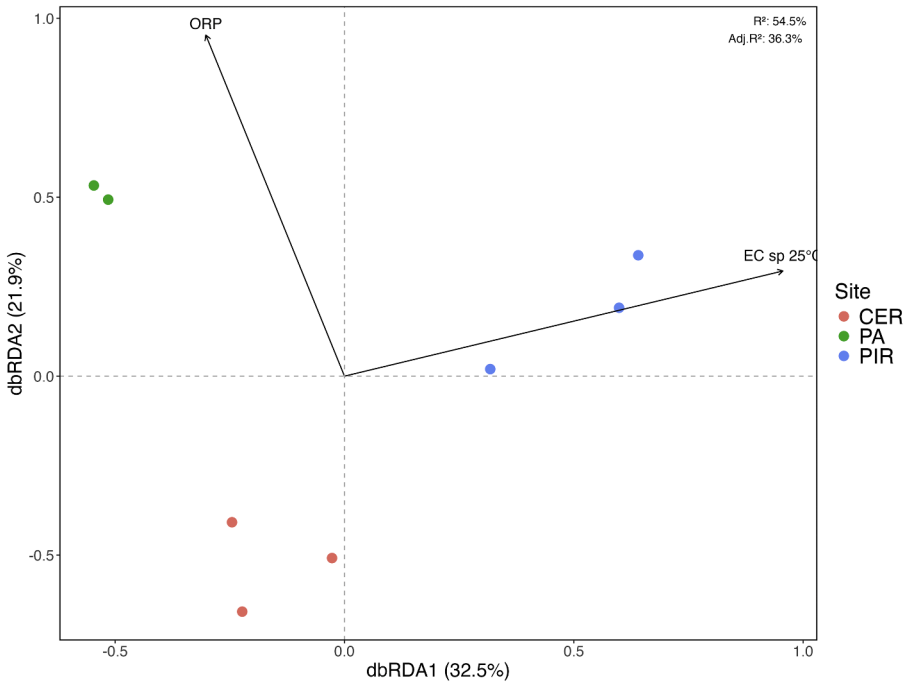

Fig. 4. Distance-based Redundancy Analysis (dbRDA) showing the relationship between microbial community structure and environmental variables across sampling sites. Arrows represent the direction and strength of environmental gradients.

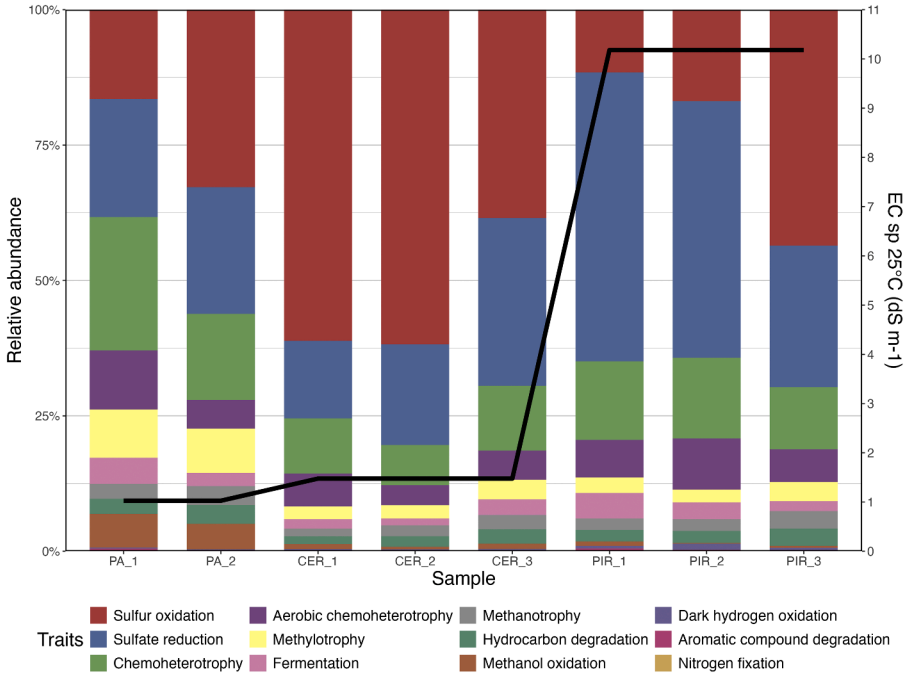

Fig. 5. Mean relative abundances of the functional groups per sampling site. Functional groups for each genus are extracted using FAPROTAX (see results) and from the cited literature (Tab. S5 in Suppl. Mat.). Shown is also the mean EC value for each sampling site (black line).

Chiapponi et al. (2024) showed that for water column depths less than 50 cm, additional constraining factors are identified, particularly the inhibitory roles of salinity and sulfate concentrations on CH_4 emissions; thus, lower fluxes of CH_4 are observed in mesohaline environments (i.e. PIR), compared to freshwater sites (PA and CER) (Tab. 1). These findings are further confirmed and integrated by the current study that gives a complementary look at how seawater presence allows SRB (Sulfate Reducing Bacteria) (Fig. 3) to outcompete methanogenic archaea for carbon substrates (Lovley and Klug, 1986), suggesting that salinity and sulfur availability drive major changes in microbial community structure in these temperate wetlands.

At the same time, recent studies highlight that the relationship between salinity and CH4 emissions is not universally negative and can vary depending on ecosystem context. Site-comparative analyses across coastal wetlands have demonstrated that CH4 responses to salinization range from negative to neutral or even positive, depending on local biogeochemical conditions and microbial community composition (Bueno De Mesquita et al., 2024). Similarly, ecosystem-scale

observations of drought-induced salinization showed that strong reductions in plant productivity were accompanied by only minor decreases in CH4 emissions, resulting in a decoupling between photosynthetic carbon inputs and CH_4 fluxes (Chamberlain et al., 2020). Vegetation responses to salinity may interact with microbial processes by modifying organic matter inputs, redox conditions, and then indirectly influencing GHG fluxes (Fei Xi et al., 2014; Li et al., 2020; Liang et al., 2025). These findings support the interpretation that salinity acts as a contextual rather than deterministic control on CH4 cycling, consistent with the patterns observed across our study sites.

The dbRDA analysis (Fig. 4) indicates that samples are organized along the salinity gradient, ranging from the freshwater site PA to the more brackish environment of PIR. This gradient is reflected in the higher EC values observed at PIR, which increase from 5.01 dS m^{-1} in the surface horizon to 12.9 dS m^{-1} in the deeper layers. In addition, PIR shows higher TOC and TN contents in the shallow horizon compared to CER and PA, suggesting enhanced organic matter availability under brackish conditions. In saline and brackish wetlands, increased sulfate availability strongly influences anaerobic carbon mineralization pathways. Sulfate acts as a preferential terminal electron acceptor, promoting sulfur cycling at the expense of methanogenesis and other redox pathways, leading to decreased CH_4 emission (Poffenbarger et al., 2011). Consistent with this mechanism, sulfate-rich environments such as PIR favor sulfate-reducing microbial communities, which outcompete methanogens for common substrates, thereby lowering CH_4 emissions (Bridgham et al., 2013; Chiapponi et al., 2024). Evidence from both natural and restored systems supports this interpretation. In hypersaline, unrestored salt ponds (151–236 ppt), very high CH_4 emissions (490–1607 μmol m^{-2} d^{-1}) were reported, likely driven by halophilic methanogens operating under conditions where sulfate is no longer limiting methanogenesis (Zhou et al., 2022). However, in restored or moderately saline systems, reduction in salinity and sulfate concentrations can shift microbial community composition toward sulfate reducers, resulting in a decrease in net CH_4 emissions. This pattern closely resembles the mesohaline conditions observed at PIR. Similarly, salinity intrusion into tidal freshwater sediments has been shown to rapidly suppress methanogenesis while increasing sulfate reduction in organic matter mineralization within a few weeks (Weston et al., 2006). Experimental studies further demonstrate that increased salinity in wetlands can reduce CH_4 emissions by about 30%, an effect attributed both to altered microbial processes and to reduced primary productivity (Neubauer, 2013).

However, studies from eutrophic and hypersaline environments show that organic matter availability and redox conditions can weaken or even counteract the inhibitory effect of salinity on CH_4 emissions. In eutrophic brackish coastal systems, high organic matter inputs combined with oxygen depletion can cause the sulfate– CH_4 transition zone to move closer to the sediment surface, reducing the effectiveness of CH_4 oxidation and allowing elevate CH_4 release (Żygadłowska et al., 2024). Similarly, in hypersaline lagoons, uneven accumulation of organic matter can lead to localized hotspots of CH_4 production despite high sulfate concentrations, especially where microbial communities rely on methylotrophic pathways using non-competitive substrates (Keneally et al., 2024). Overall, these studies indicate that organic matter supply and redox conditions play a key role in controlling CH_4 emissions along salinity gradients.

The freshwater site PA was dominated by *Synthrophus* (Fig. 3b), whose presence is linked to CH_4 production through syntrophic interactions with methanogenic archaea. *Syntrophus* degrades organic matter (high in content in PA as indicated in Tab. 2) into smaller molecules (e.g., H_2, and CO_2), which are subsequently consumed by methanogens to produce CH_4 (Berrier et al., 2022).

The low EC recorded in PA may explain the almost absence of *Haliangium*, a salt-tolerant myxobacteria found in saline and riparian soils (Fudou et al., 2002) and known to have a selective predation for methanotrophs (Kaupper et al., 2022). The highest ORP values and the lowest AVS values measured in PA compared to the other sites (Tab. 2) suggest a less reduced environment with lower sulfide content and it could explain the presence of *Thiobacillus.* These bacteria are aerobic or facultatively anaerobic sulfur oxidizers (Bosecker, 1997; Johnson et al., 2013) that can use ferric iron as an alternative electron acceptor under anoxic conditions (Brandl, 2001; Rawlings, 2002).

In contrast, the microbial community structure at CER shows the highest species richness among all sites. The presence of *Thiobacillus, Sulfuricurvum*, and *Sulfuricaulis* indicate that the CER ecosystem is involved, not only in sulfur cycling, but also in carbon fixation and nitrogen cycling through chemolithoautotrophic growth coupled to nitrate or oxygen reduction, whereas *Lysobacter* primarily participates in organic matter degradation and nutrient recycling. The presence of *Lysobacter* seems related to high concentration of Fe(III) since this genus is linked to its presence in soils. *Sulfuricurvum* and *Sulfuricaulis,* like-*Thiobacillus,* are sulfur oxidizing bacteria (SOBs) that are involved in the oxidation of sulfur compounds and the production of sulfuric acid (Haaijer et al., 2008). These bacteria may be present in soils with high sulfur concentrations (She et al., 2016), like the ones we find both in the topmost (0-5 cm) and the deepest (23-35+ cm) horizons of CER (Tab. 2). *Thiobacillus* species may be key players in nitrate-dependent iron sulfide dissolution in freshwater wetlands (Haaijer et al., 2008); nitrate acts as an electron acceptor in the dissolution of iron sulfide, leading to the production of Fe(III), N_2 and sulfate. Depending on environmental conditions and the available compounds, alternative or intermediate reactions involving reduced nitrogen species such as nitrite or ammonium may also occur.

A distinct shift in the microbial community structure is observable at the brackish-water site PIR, where sulfate-reducing bacteria such as *Desulfatiglans* and *Desulfosarcina* dominate, together with *Algorimarina* and *Thiobacillus* (Fig. 3b). The differences in microbial community, compared to PA and CER, imply that the brackish-water site PIR has a distinct microbial community structure, with distinct taxa dominating each sample. In this specific context, these sulfate-reducing bacteria (SRB) play a key role in sulfur metabolism, reducing sulfate to sulfide under anoxic conditions and have been shown to be important decomposer communities in coastal salt marsh sediments (Jackson et al., 2014). Their activity can contribute to the reduction of sulfate near the sediment-water interface, leading to the precipitation of iron sulphides and affecting the cycling of iron and sulfur in the wetland (Fortin et al., 2000). *Anaerohalosphaera* is a genus containing obligately anaerobic, moderately halophilic and mesophilic taxa that can assimilate sulfate (Pradel et al., 2020).

Candry et al. (2023) demonstrated that sulfate-reducing microbes can outcompete methanogens for organic carbon, favouring the production of CO_2 and leading to lower CH_4 emissions in wetlands. Consistently, Chiapponi et al. (2024) showed that PIR sites exhibit low CH_4 and high CO_2 fluxes, comparable to those observed in freshwater environments, particularly CER, as indicated by the low CH_4/CO_2 volumetric ratio (Tab. 1). Similar patterns were observed in other studies showing that high salinity and atmospheric CO_2 increase the SRB abundance without eliminating methanogens (Kim et al., 2020), while still decreasing CH_4 emissions (Poffenbarger et al., 2011).

Microbial pathway shifts provide a mechanistic framework to interpret these observations. Experimental evidence from hypersaline wetlands shows that methylotrophic methanogenesis can persist within sulfate-rich sediments, while CH_4 is simultaneously consumed through anaerobic oxidation coupled to sulfate or alternative electron acceptors such as iron, resulting in low net CH_4 accumulation (Krause and Treude, 2021). This “cryptic methane cycle” suggests that low CH_4 emissions do not necessarily indicate suppressed methanogenesis, but rather efficient internal recycling of CH_4.

SRB competition may also increase CO_2 emissions, potentially offsetting the climatic benefits of reduced CH_4 emissions and the carbon sink capacity of wetlands (La et al., 2022; Pester, 2012). Also, it is known that regular changes in soil redox conditions caused by dry-wet

transitions can reduce CH_4 output while increasing N_2O emissions at the same time, offsetting the advantages of CH_4 mitigation, too (Peyron et al., 2016). Such dynamics may be particularly relevant in these human-managed wetlands, where water levels, flooding duration, and seasonal management differ markedly among sites: PIR is a pond with undefined banks, permanently flooded with considerable seasonal differences in water level; PA is almost permanently flooded and water recharge is often stopped in summer (June-August) when the mowing of the halophytic vegetation is performed; while CER, being located in an interdunal area, gets partly dry in summer, when the water table decreases and evaporation increases.

Despite the high abundance of sulfur-cycling taxa, FAPROTAX analysis also revealed low-abundance functional groups related to methanotrophy, methanol oxidation and methylotrophy, particularly at PA site. Since targeted gene quantifications (e.g., qPCR/qRT-PCR of mcrA/pmoA) were not performed, FAPROTAX data should be taken with caution. Nevertheless, the low abundance of methanogens, could likely reflect the shallow sampling depth (20 cm), where partial oxygenation from the overlying water column limits the anoxic conditions typical of deeper soil layers; nevertheless, their methanogenic activity can remain ecologically important even when they constitute only a small fraction of the community (Angle et al., 2017).

Furthermore, the complexity of the microbial community composition in the samples needs to be taken into consideration. If these organisms are present in low abundance compared to the overall microbial pool, they may face competition during amplification, leading to their exclusion in sequencing results and falling below the Nanopore detection limit (90 CFU/ml) (Lao et al., 2024). Additionally, the choice of primers plays a crucial role, as some studies recommend using archaeal-specific primers to ensure proper amplification (Akaçin et al., 2023; Lao et al., 2024). These technical issues, combined with the fact that the metabolic function was only inferred through FAPROTAX, the detection of methanogens and other archaea could be underestimated.

Further studies at higher vertical resolution (i.e., at each pedological-horizon level) and involving more control replicates and specific functional assays can be done to better investigate the presence and role of methanogens in these complex environments. Overall, our results represent a site-specific but ecologically meaningful case study that can inform future multi-site research that at the moment are limited for temperate coastal wetlands.

5. Conclusion

In this study, we investigate the microbial communities at three managed temperate coastal wetlands of the Northern Adriatic coast (Italy) along a salinity gradient to assess the interplay between biogeochemical processes in soil and GHG emissions. By characterizing microbial communities involved in carbon mineralization under field conditions, this work addresses a gap in empirical data for temperate Mediterranean coastal wetlands, where microbial ecology, soil geochemistry, and GHG fluxes are rarely investigated together. A key contribution of this study is the integrated approach, combining soil physicochemical and pedological characterization, 16S rRNA gene sequencing metabarcoding of microbial communities, sulfur- and redox-related geochemistry, and in situ measurements of CO_2 and CH_4 fluxes at the same sites. This allows us to move beyond general assumptions, such as a simple inhibitory effect of salinity on CH_4 emission, and to identify which microbial groups dominate along the salinity gradient, which metabolic pathways are favored, and how these shifts correspond to contrasting CO_2–CH_4 emission patterns.

The results suggest that EC and S availability are major drivers of microbial community structure across sites. The clustering analysis reveals three distinct community types: freshwater communities; taxa associated with shallow-freshwater conditions, and community characteristics of brackish environments. In freshwater ecosystems (PA and CER), sulfur-oxidizing bacteria (SOB) dominate, while in brackish environments (PIR), sulfate-reducing bacteria (SRB) are prevalent. High salinity and elevated Fe concentrations at the brackish-water site drive a shift in microbial communities towards an abundance of SRB, which outcompete methanogens for organic carbon substrates, leading to a decrease in CH_4 emissions and an increase in CO_2 production.

Microbial community composition reflects soil conditions shaped by long-term salinity and redox regimes, while GHG fluxes represent the integrated outcome of these processes at the site scale rather than direct, short-term responses to specific microbial groups. By relating microbial patterns to long-term, site-integrated flux regimes instead of instantaneous measurements, this study accounts for the strong spatial and temporal variability that characterizes GHG emissions in coastal wetlands.

Overall, this work provides a site-specific but ecologically relevant case study that supports growing evidence from coastal systems showing that CH_4 dynamics along salinity gradients are controlled by the interaction between organic matter availability, redox conditions, and microbial functional pathways, rather than by salinity alone.

While acknowledging the study limited application and the complex nature of wetland systems, the results also point to a potential trade-off under increasing salinization, where lower CH_4 emissions may be accompanied by higher CO_2 emissions, potentially reducing the net carbon sink capacity of wetlands. From a management perspective, these findings stress the importance of considering the full GHG balance when evaluating wetland responses to salinization and climate-driven changes such as sea-level rise and saltwater intrusion.

Funding

This study was carried out within the RETURN Extended Partnership and received funding from the European Union Next-GenerationEU (National Recovery and Resilience Plan – NRRP, Mission 4, Component 2, Investment 1.3 – D.D. 1243 2/8/2022, PE0000005).

CRediT authorship contribution statement

Emilia Chiapponi: Writing – original draft, Visualization, Software, Methodology, Investigation, Formal analysis, Data curation. **Beatrice Maria Sole Giambastiani:** Writing – review & editing, Visualization, Validation, Supervision, Investigation, Data curation, Conceptualization. **Nicolas Greggio:** Writing – review & editing, Methodology, Formal analysis. **Denis Zannoni:** Methodology, Formal analysis, Data curation. **Sonia Silvestri:** Validation, Supervision, Investigation, Funding acquisition, Data curation, Conceptualization. **Alessandro Buscaroli:** Writing – review & editing, Validation, Investigation, Data curation. **Alessandro Piazza:** Visualization, Data curation, Software. **Federica Costantini:** Writing – review & editing, Validation, Supervision, Software, Methodology, Data curation, Conceptualization.

Declaration of competing interest

The authors declare that they have no known competing financial interests or personal relationships that could have appeared to influence the work reported in this paper.

Acknowledgment

This study was performed with the support of the Ravenna municipality (Italy) that granted access to the reserve and the support of the Office for Biodiversity Protection of Punta Marina (Carabinieri Forestali). The authors would like to thank Dr. Francesco Mugnai and Dr. Martina La Torre for their support during the metagenomics analysis and Prof. Enrico Dinelli for performing XRF analysis on samples.

Supplementary materials

Supplementary material associated with this article can be found, in the online version, at doi:10.1016/j.envadv.2026.100698.

Data availability

Raw metabarcoding data and metadata used for this research are available at this address: 10.5281/zenodo.18270967.

References

Akaçin, İ., Ersoy, Ş., Doluca, O., Güngörmüşler, M., 2023. Using custom-built primers and nanopore sequencing to evaluate CO-utilizer bacterial and archaeal populations linked to bioH2 production. Sci. Rep. 13, 17025. https://doi.org/10.1038/s41598-023-44357-3.

An, L., Yan, Y.C., Tian, H.L., Chi, C.Q., Nie, Y., Wu, X.L., 2023. Roles of sulfate-reducing bacteria in sustaining the diversity and stability of marine bacterial community. Front. Microbiol. 14, 1218828. https://doi.org/10.3389/fmicb.2023.1218828.

Angle, J.C., Morin, T.H., Solden, L.M., Narrowe, A.B., Smith, G.J., Borton, M.A., Rey-Sanchez, C., Daly, R.A., Mirfenderesgi, G., Hoyt, D.W., Riley, W.J., Miller, C.S., Bohrer, G., Wrighton, K.C., 2017. Methanogenesis in oxygenated soils is a substantial fraction of wetland methane emissions. Nat. Commun. 8, 1567. https://doi.org/10.1038/s41467-017-01753-4.

Antonellini, M., Giambastiani, B.M.S., Greggio, N., Bonzi, L., Calabrese, L., Luciani, P., Perini, L., Severi, P., 2019. Processes governing natural land subsidence in the shallow coastal aquifer of the Ravenna coast, Italy. CATENA 172, 76–86. https://doi.org/10.1016/j.catena.2018.08.019.

Antonellini, M., Mollema, P., Giambastiani, B., Bishop, K., Caruso, L., Minchio, A., Pellegrini, L., Sabia, M., Ulazzi, E., Gabbianelli, G., 2008. Salt water intrusion in the coastal aquifer of the southern Po Plain, Italy. Hydrogeol. J. 16, 1541–1556. https://doi.org/10.1007/s10040-008-0319-9.

Bartlett, K.B., Bartlett, D.S., Harriss, R.C., Sebacher, D.I., 1987. Methane emissions along a salt marsh salinity gradient. Biogeochemistry 4, 183–202. https://doi.org/10.1007/BF02187365.

Berrier, D.J., Neubauer, S.C., Franklin, R.B., 2022. Cooperative microbial interactions mediate community biogeochemical responses to saltwater intrusion in wetland soils. FEMS Microbiol. Ecol. 98. https://doi.org/10.1093/femsec/fiac019 fiac019.

Bonetti, G., Trevathan-Tackett, S.M., Carnell, P.E., Treby, S., Macreadie, P.I., 2021. Local vegetation and hydroperiod influence spatial and temporal patterns of carbon and microbe response to wetland rehabilitation. Appl. Soil Ecol. 163, 103917. https://doi.org/10.1016/j.apsoil.2021.103917.

Bosecker, K., 1997. Bioleaching: metal solubilization by microorganisms. FEMS Microbiol. Rev. 20, 591–604. https://doi.org/10.1111/j.1574-6976.1997.tb00340.x.

Brandl, H., 2001. Microbial leaching of metals. In: Rehm, H.J., Reed, G. (Eds.), Biotechnology Set. Wiley, pp. 191–224. https://doi.org/10.1002/9783527620999.ch8k.

Bridgham, S.D., Cadillo-Quiroz, H., Keller, J.K., Zhuang, Q., 2013. Methane emissions from wetlands: biogeochemical, microbial, and modeling perspectives from local to global scales. Glob. Change Biol. 19, 1325–1346. https://doi.org/10.1111/gcb.12131.

Bueno De Mesquita, C.P., Hartman, W.H., Ardón, M., Bernhardt, E.S., Neubauer, S.C., Weston, N.B., Tringe, S.G., 2024. Microbial ecology and site characteristics underlie differences in salinity-methane relationships in coastal wetlands. JGR Biogeosciences 129, e2024JG008133. https://doi.org/10.1029/2024JG008133.

Buscaroli, A., Gherardi, M., Vianello, G., Vittori Antisari, L., Zannoni, D., 2009. Soil survey and classification in a complex territorial system: Ravenna (italy). EQA Int. J. Environ. Qual. 2, 15–28. https://doi.org/10.6092/ISSN.2281-4485/3815. Vol.

Buscaroli, A., Zannoni, D., 2017. Soluble ions dynamics in Mediterranean coastal pinewood forest soils interested by saline groundwater. CATENA 157, 112–129. https://doi.org/10.1016/j.catena.2017.05.014 (Amst).

Buscaroli, A., Zannoni, D., 2010. Influence of ground water on soil salinity in the San Vitale Pinewood (Ravenna - Italy) Vol. LIV-N. 5.

Candry, P., Abrahamson, B., Stahl, D.A., Winkler, M.H., 2023. Microbially mediated climate feedbacks from wetland ecosystems. Glob. Change Biol. 29, 5169–5183. https://doi.org/10.1111/gcb.16850.

Capone, D.G., Kiene, R.P., 1988. Comparison of microbial dynamics in marine and freshwater sediments: contrasts in anaerobic carbon catabolism1. Limnol. Oceanogr. 33, 725–749. https://doi.org/10.4319/lo.1988.33.4part2.0725.

Chamberlain, S.D., Hemes, K.S., Eichelmann, E., Szutu, D.J., Verfaillie, J.G., Baldocchi, D.D., 2020. Effect of drought-induced salinization on wetland methane emissions, gross ecosystem productivity, and their interactions. Ecosystems 23, 675–688. https://doi.org/10.1007/s10021-019-00430-5.

Chen, Y., Wu, N., Liu, C., Mi, T., Li, J., He, X., Li, S., Sun, Z., Zhen, Y., 2022. Methanogenesis pathways of methanogens and their responses to substrates and temperature in sediments from the South Yellow Sea. Sci. Total Environ. 815, 152645. https://doi.org/10.1016/j.scitotenv.2021.152645.

Chiapponi, E., Silvestri, S., Zannoni, D., Antonellini, M., Giambastiani, B.M.S., 2024. Driving and limiting factors of CH 4 and CO 2 emissions from coastal brackish-water wetlands in temperate regions (preprint). Biogeochemistry: Wetlands. 10.5194/egusphere-2023-605.

Clarke, K.R., 1993. Non-parametric multivariate analyses of changes in community structure. Aust. J. Ecol. 18, 117–143. https://doi.org/10.1111/j.1442-9993.1993.tb00438.x.

Clarke, K.R., Gorley, R.N., 2015. PRIMER v7: User Manual/Tutorial.

Council Directive 92/43/EEC of 21 May 1992 on the conservation of natural habitats and of wild fauna and flora, 1992.

Directive 2009/147/EC of the European Parliament and of the Council of 30 November 2009 on the conservation of wild birds (Codified version), 2010.

Duarte, C.M., Losada, I.J., Hendriks, I.E., Mazarrasa, I., Marbà, N., 2013. The role of coastal plant communities for climate change mitigation and adaptation. Nat. Clim Change 3, 961–968. https://doi.org/10.1038/nclimate1970.

Fei Xi, X., Wang, L., Jun Hu, J., Shu Tang, Y., Hu, Y., Hua Fu, X., Sun, Y., Fai Tsang, Y., Nan Zhang, Y., Hai Chen, J., 2014. Salinity influence on soil microbial respiration rate of wetland in the Yangtze River estuary through changing microbial community. J. Environ. Sci. 26, 2562–2570. https://doi.org/10.1016/j.jes.2014.07.016.

Ferronato, C., Falsone, G., Natale, M., Zannoni, D., Buscaroli, A., Vianello, G., Vittori Antisari, L., 2016. Chemical and pedological features of subaqueous and hydromorphic soils along a hydrosequence within a coastal system (San Vitale Park, Northern Italy). Geoderma 265, 141–151. https://doi.org/10.1016/j.geoderma.2015.11.018.

Fortin, D., Goulet, R., Roy, M., 2000. Seasonal cycling of Fe and s in a constructed wetland: the role of sulfate-reducing bacteria. Geomicrobiol. J. 17, 221–235. https://doi.org/10.1080/01490450050121189.

Fudou, R., Jojima, Y., Iizuka, T., Yamanaka, S., 2002. Haliangium ochraceum gen. nov., sp. nov. and Haliangium tepidum sp. nov.: Novel moderately halophilic myxobacteria isolated from coastal saline environments. J. Gen. Appl. Microbiol. 48, 109–115. https://doi.org/10.2323/jgam.48.109.

Giambastiani, B.M.S., Antonellini, M., Oude Essink, G.H.P., Stuurman, R.J., 2007. Saltwater intrusion in the unconfined coastal aquifer of Ravenna (Italy): a numerical model. J. Hydrol. 340, 91–104. https://doi.org/10.1016/j.jhydrol.2007.04.001 (Amst).

Giambastiani, B.M.S., Kidanemariam, A., Dagnew, A., Antonellini, M., 2021. Evolution of salinity and water table level of the phreatic coastal aquifer of the Emilia Romagna region (Italy). Water 13, 372. https://doi.org/10.3390/w13030372 (Basel).

Giambastiani, B.M.S., Macciocca, V.R., Molducci, M., Antonellini, M., 2020. Factors affecting water drainage long-time series in the salinized low-lying coastal area of Ravenna (Italy). Water 12, 256. https://doi.org/10.3390/w12010256 (Basel).

Gillanders, B., Kingsford, M., 2002. Impact of changes in flow of freshwater on estuarine and open coastal habitats and the associated organisms. In: Atkinson, R., Barnes, M. (Eds.), Oceanography and Marine Biology, An Annual Review, Volume 40, Oceanography and Marine Biology - An Annual Review. CRC Press, pp. 233–309. https://doi.org/10.1201/9780203180594.ch5.

González-Ortegón, E., Baldó, F., Arias, A., Cuesta, J.A., Fernández-Delgado, C., Vilas, C., Drake, P., 2015. Freshwater scarcity effects on the aquatic macrofauna of a European Mediterranean-climate estuary. Sci. Total Environ. 503–504, 213–221. https://doi.org/10.1016/j.scitotenv.2014.06.020.

Haaijer, S.C.M., Harhangi, H.R., Meijerink, B.B., Strous, M., Pol, A., Smolders, A.J.P., Verwegen, K., Jetten, M.S.M., Op Den Camp, H.J.M., 2008. Bacteria associated with iron seeps in a sulfur-rich, neutral pH, freshwater ecosystem. ISMe J. 2, 1231–1242. https://doi.org/10.1038/ismej.2008.75.

Hach Company, 2019. Sulfate, SulfaVer 4 Method (70 mg/L).

Hartman, W.H., Bueno De Mesquita, C.P., Theroux, S.M., Morgan-Lang, C., Baldocchi, D. D., Tringe, S.G., 2024. Multiple microbial guilds mediate soil methane cycling along a wetland salinity gradient. mSystems 9. https://doi.org/10.1128/msystems.00936-23 e00936-23.

Hopkinson, C.S., Cai, W.J., Hu, X., 2012. Carbon sequestration in wetland dominated coastal systems—a global sink of rapidly diminishing magnitude. Curr. Opin. Environ. Sustain. 4, 186–194. https://doi.org/10.1016/j.cosust.2012.03.005.

International Standard Organization, S., 1995. ISO 10694:1995, Soil quality - Determination of organic and total carbon after dry combustion (elementary analysis) Technical Committee ISO/TC 190.

IPCC - Intergovernmental Panel On Climate Change (Ipcc), 2022. The Ocean and Cryosphere in a Changing Climate: Special Report of the Intergovernmental Panel on Climate Change, 1st ed. Cambridge University Press. https://doi.org/10.1017/9781009157964.

Jackson, K.L., Whitcraft, C.R., Dillon, J.G., 2014. Diversity of desulfobacteriaceae and overall activity of sulfate-reducing microorganisms in and around a salt pan in a southern California coastal Wetland. Wetlands 34, 969–977. https://doi.org/10.1007/s13157-014-0560-z.

Johnson, D., Grail, B., Hallberg, K., 2013. A new direction for biomining: extraction of metals by reductive dissolution of oxidized ores. Minerals 3, 49–58. https://doi.org/10.3390/min3010049.

Jørgensen, B.B., Findlay, A.J., Pellerin, A., 2019. The biogeochemical sulfur cycle of marine sediments. Front. Microbiol. 10, 849. https://doi.org/10.3389/fmicb.2019.00849.

Kasozi, G.N., Nkedi-Kizza, P., Harris, W.G., 2009. Varied carbon content of organic matter in histosols, spodosols, and Carbonatic Soils. Soil. Sci. Soc. Am. J. 73, 1313–1318. https://doi.org/10.2136/sssaj2008.0070.

Kaupper, T., Mendes, L.W., Poehlein, A., Frohloff, D., Rohrbach, S., Horn, M.A., Ho, A., 2022. The methane-driven interaction network in terrestrial methane hotspots. Environ. Microbiome 17, 15. https://doi.org/10.1186/s40793-022-00409-1.

Keneally, C., Southgate, M., Chilton, D., Gaget, V., Welsh, D.T., Mosley, L., Erler, D.V., Kidd, S.P., Brookes, J., 2024. Organic matter accumulation drives methylotrophic methanogenesis and microbial ecology in a hypersaline coastal lagoon. Limnol. Oceanogr. 69, 1970–1983. https://doi.org/10.1002/lno.12637.

Kerkhof, L.J., Dillon, K.P., Häggblom, M.M., McGuinness, L.R., 2017. Profiling bacterial communities by MinION sequencing of ribosomal operons. Microbiome 5, 116. https://doi.org/10.1186/s40168-017-0336-9.

Kim, S.Y., Freeman, C., Lukac, M., Lee, S.H., Kim, S.D., Kang, H., 2020. Elevated CO2 and high salinity enhance the abundance of sulfate reducers in a salt marsh ecosystem. Appl. Soil Ecol. 147, 103386. https://doi.org/10.1016/j.apsoil.2019.103386.

Krause, S.J.E., Treude, T., 2021. Deciphering cryptic methane cycling: coupling of methylotrophic methanogenesis and anaerobic oxidation of methane in hypersaline coastal wetland sediment. Geochim. Cosmochim. Acta 302, 160–174. https://doi.org/10.1016/j.gca.2021.03.021.

Kumari, K., Naskar, M., Aftabuddin, Md., Sarkar, U.K., Nag, S.K., Ghosh, B.D., Das, B.K., 2025. Assessment of three prokaryote primers for concurrent and comprehensive profiling of methanogen and methanotroph community and habitat specificity in three distinct wetland sediments. J. Soils Sediments 25, 2112–2125. https://doi.org/10.1007/s11368-025-04061-3.

La, W., Han, X., Liu, C.Q., Ding, H., Liu, M., Sun, F., Li, S., Lang, Y., 2022. Sulfate concentrations affect sulfate reduction pathways and methane consumption in coastal wetlands. Water Res. 217, 118441. https://doi.org/10.1016/j.watres.2022.118441.

Lao, H.Y., Wong, L.L.Y., Hui, Y., Ng, T.T.L., Chan, C.T.M, Lo, H.W.H, Yau, M.C.Y, Leung, E.C.M, Wong, R.C.W, Ho, A.Y.M, Yip, K.T, Lam, J.Y.W, Chow, V.C.Y, Luk, K.S, Que, T.L, Chow, F.W.N, Siu, G.K.H, 2024. The clinical utility of Nanopore 16S rRNA gene sequencing for direct bacterial identification in normally sterile body fluids. Front. Microbiol. 14, 1324494. https://doi.org/10.3389/fmicb.2023.1324494.

Li, Y.L., Guo, H.Q., Ge, Z.M., Wang, D.Q., Liu, W.L., Xie, L.N., Li, S.H., Tan, L.S., Zhao, B., Li, X.Z., Tang, J.W., 2020. Sea-level rise will reduce net CO2 uptake in subtropical coastal marshes. Sci. Total Environ. 747, 141214. https://doi.org/10.1016/j.scitotenv.2020.141214.

Liang, S., Li, H., Wu, H., Yan, B., Song, A., 2023. Microorganisms in coastal wetland sediments: a review on microbial community structure, functional gene, and environmental potential. Front. Microbiol. 14, 1163896. https://doi.org/10.3389/fmicb.2023.1163896.

Liang, Z., Song, J., Li, X., Zhao, M., Chu, X., Wang, X., Li, P., Zhang, X., Song, W., Wei, S., Sun, R., Jiang, C., Han, G., 2025. Plant life form determines net ecosystem CO2 exchange in a salt marsh under precipitation changes. Agric. For. Meteorol. 369, 110572. https://doi.org/10.1016/j.agrformet.2025.110572.

Louca, S., Parfrey, L.W., Doebeli, M., 2016. Decoupling function and taxonomy in the global ocean microbiome. Science 353, 1272–1277. https://doi.org/10.1126/science.aaf4507 (1979).

Lovley, D.R., Klug, M.J., 1986. Model for the distribution of sulfate reduction and methanogenesis in freshwater sediments. Geochim. Cosmochim. Acta 50, 11–18. https://doi.org/10.1016/0016-7037(86)90043-8.

Marani, M., D'Alpaos, A., Lanzoni, S., Carniello, L., Rinaldo, A., 2010. The importance of being coupled: stable states and catastrophic shifts in tidal biomorphodynamics. J. Geophys. Res. 115. https://doi.org/10.1029/2009JF001600, 2009JF001600.

Marani, M., Zillio, T., Belluco, E., Silvestri, S., Maritan, A., 2006. Non-neutral vegetation dynamics. PLoS One 1, e78. https://doi.org/10.1371/journal.pone.0000078.

McCuen, M.M., Pitesky, M.E., Buler, J.J., Acosta, S., Wilcox, A.H., Bond, R.F., Díaz-Muñoz, S.L., 2021. A comparison of amplification methods to detect Avian Influenza viruses in California wetlands targeted via remote sensing of waterfowl. Transbound. Emerg. Dis. 68, 98–109. https://doi.org/10.1111/tbed.13612.

Neubauer, S.C., 2013. Ecosystem responses of a tidal freshwater marsh experiencing saltwater intrusion and altered hydrology. Estuaries Coasts 36, 491–507. https://doi.org/10.1007/s12237-011-9455-x.

Oksanen, J., Simpson, G., Blanchet, F., Kindt, R., Legendre, P., Minchin, P., O'Hara, R., Solymos, P., Stevens, M., Szoecs, E., Wagner, H., Barbour, M., Bedward, M., Bolker, B., Borcard, D., Carvalho, G., Chirico, M., De Caceres, M., Durand, S., Evangelista, H., FitzJohn, R., Friendly, M., Furneaux, B., Hannigan, G., Hill, M., Lahti, L., McGlinn, D., Ouellette, M., Ribeiro Cunha, E., Smith, T., Stier, A., Ter Braak, C., Weedon, J., 2022. . vegan: community ecology package. R package.

Pellegrini, E., Contin, M., Vittori Antisari, L., Vianello, G., Ferronato, C., De Nobili, M., 2018. A new paper sensor method for field analysis of acid volatile sulfides in soils: paper sensor method for field analysis of acid volatile sulfides. Environ. Toxicol. Chem. 37, 3025–3031. https://doi.org/10.1002/etc.4279.

Pester, M., 2012. Sulfate-reducing microorganisms in wetlands – fameless actors in carbon cycling and climate change. Front. Microbiol. 3. https://doi.org/10.3389/fmicb.2012.00072.

Peyron, M., Bertora, C., Pelissetti, S., Said-Pullicino, D., Celi, L., Miniotti, E., Romani, M., Sacco, D., 2016. Greenhouse gas emissions as affected by different water management practices in temperate rice paddies. Agric. Ecosyst. Environ. 232, 17–28. https://doi.org/10.1016/j.agee.2016.07.021.

Pielou, E.C., 1966. The measurement of diversity in different types of biological collections. J. Theor. Biol. 13, 131–144. https://doi.org/10.1016/0022-5193(66)90013-0.

Poffenbarger, H.J., Needelman, B.A., Megonigal, J.P., 2011. Salinity influence on methane emissions from tidal marshes. Wetlands 31, 831–842. https://doi.org/10.1007/s13157-011-0197-0.

Pradel, N., Fardeau, M.L., Tindall, B.J., Spring, S., 2020. Anaerohalosphaera lusitana gen. nov., sp. nov., and Limihaloglobus sulfuriphilus gen. nov., sp. nov., isolated from solar saltern sediments, and proposal of Anaerohalosphaeraceae fam. nov. within the order Sedimentisphaerales. Int. J. Syst. Evol. Microbiol. 70, 1321–1330. https://doi.org/10.1099/ijsem.0.003919.

Pruesse, E., Peplies, J., Glöckner, F.O., 2012. SINA: Accurate high-throughput multiple sequence alignment of ribosomal RNA genes. Bioinformatics 28, 1823–1829. https://doi.org/10.1093/bioinformatics/bts252.

Rawlings, D.E., 2002. Heavy metal mining using microbes. Annu. Rev. Microbiol. 56, 65–91. https://doi.org/10.1146/annurev.micro.56.012302.161052.

Salimi, S., Almuktar, S.A.A.A.N., Scholz, M., 2021. Impact of climate change on wetland ecosystems: a critical review of experimental wetlands. J. Environ. Manage 286, 112160. https://doi.org/10.1016/j.jenvman.2021.112160.

Sansupa, C., Wahdan, S.F.M., Hossen, S., Disayathanoowat, T., Wubet, T., Purahong, W., 2021. Can we use functional annotation of prokaryotic taxa (FAPROTAX) to assign the ecological functions of soil bacteria? Appl. Sci. 11, 688. https://doi.org/10.3390/app11020688.

Sayers, E.W., Bolton, E.E., Brister, J.R., Canese, K., Chan, J., Comeau, D.C., Connor, R., Funk, K., Kelly, C., Kim, S., Madej, T., Marchler-Bauer, A., Lanczycki, C., Lathrop, S., Lu, Z., Thibaud-Nissen, F., Murphy, T., Phan, L., Skripchenko, Y., Tse, T., Wang, J., Williams, R., Trawick, B.W., Pruitt, K.D., Sherry, S.T., 2022. Database resources of the national center for biotechnology information. Nucleic Acids Res. 50, D20–D26. https://doi.org/10.1093/nar/gkab1112.

She, C.X., Zhang, Z.C., Cadillo-Quiroz, H., Tong, C., 2016. Factors regulating community composition of methanogens and sulfate-reducing bacteria in brackish marsh sediments in the Min River estuary, southeastern China. Estuar. Coast. Shelf Sci. 181, 27–38. https://doi.org/10.1016/j.ecss.2016.08.003.

Soil Survey Staff, 2022. Keys to Soil Taxonomy, 13th edition. ed. USDA natural resources conservation service.

Trettin, C.C., Jurgensen, M.F., Dai, Z., 2019. Effects of climate change on forested wetland soils. Developments in Soil Science. Elsevier, pp. 171–188. https://doi.org/10.1016/B978-0-444-63998-1.00009-4.

Wallenius, A.J., Venetz, J., Zygadlowska, O.M., Lenstra, W.K., van Helmond, N.A.G.M., Dalcin Martins, P., Slomp, C.P., Jetten, M.S.M., 2025. A ubiquitous and diverse methanogenic community drives microbial methane cycling in eutrophic coastal sediments. FEMS Microbiol. Ecol. 101. https://doi.org/10.1093/femsec/fiaf075 fiaf075.

Weingarten, E.A., Jung, C.M., Crocker, F.H., Kneer, M.L., Hurst, N.R., Chappell, M.A., Berkowitz, J.F., Indest, K.J., 2023. Connecting coastal wetland microbial community characteristics with soil physicochemical properties across an estuarine salinity and vegetation gradient in Mobile Bay, AL, USA. Front. Mar. Sci. 10, 1304624. https://doi.org/10.3389/fmars.2023.1304624.

Weston, N.B., Dixon, R.E., Joye, S.B., 2006. Ramifications of increased salinity in tidal freshwater sediments: geochemistry and microbial pathways of organic matter mineralization. J. Geophys. Res. 111. https://doi.org/10.1029/2005JG000071, 2005JG000071.

White, E., Kaplan, D., 2017. Restore or retreat? saltwater intrusion and water management in coastal wetlands. Ecosyst. Health Sustain. 3, e01258. https://doi.org/10.1002/ehs2.1258.

Wood, D.E., Lu, J., Langmead, B., 2019. Improved metagenomic analysis with Kraken 2. Genome Biol. 20, 257. https://doi.org/10.1186/s13059-019-1891-0.

Yang, Z., Tognin, D., Finotello, A., Belluco, E., Puppin, A., Silvestri, S., Marani, M., D'Alpaos, A., 2023. Long-term monitoring of coupled vegetation and elevation changes in response to sea level rise in a microtidal salt marsh. JGR Biogeosciences 128. https://doi.org/10.1029/2023JG007405 e2023JG007405.

Yousefi Lalimi, F., Silvestri, S., D'Alpaos, A., Roner, M., Marani, M., 2018. The spatial variability of organic matter and decomposition processes at the marsh scale. JGR Biogeosciences 123, 3713–3727. https://doi.org/10.1029/2017JG004211.

Zhang, G., Bai, J., Tebbe, C.C., Zhao, Q., Jia, J., Wang, W., Wang, X., Yu, L., 2021. Salinity controls soil microbial community structure and function in coastal estuarine wetlands. Environ. Microbiol. 23, 1020–1037. https://doi.org/10.1111/1462-2920.15281.

Zhao, J., Chakrabarti, S., Chambers, R., Weisenhorn, P., Travieso, R., Stumpf, S., Standen, E., Briceno, H., Troxler, T., Gaiser, E., Kominoski, J., Dhillon, B., Martens-Habbena, W., 2023. Year-around survey and manipulation experiments reveal differential sensitivities of soil prokaryotic and fungal communities to saltwater intrusion in Florida Everglades wetlands. Sci. Total Environ. 858, 159865. https://doi.org/10.1016/j.scitotenv.2022.159865.

Zhou, J., Theroux, S.M., Bueno De Mesquita, C.P., Hartman, W.H., Tian, Y., Tringe, S.G., 2022. Microbial drivers of methane emissions from unrestored industrial salt ponds. ISMe J. 16, 284–295. https://doi.org/10.1038/s41396-021-01067-w.

Żygadłowska, O.M., Roth, F., Van Helmond, N.A.G.M., Lenstra, W.K., Venetz, J., Dotsios, N., Röckmann, T., Veraart, A.J., Stranne, C., Humborg, C., Jetten, M.S.M., Slomp, C.P., 2024. Eutrophication and deoxygenation drive high methane emissions from a brackish coastal system. Environ. Sci. Technol. 58, 10582–10590. https://doi.org/10.1021/acs.est.4c00702.